NASA Technical Paper 3458

1994

Results of a Laboratory Experiment That Tests Rotating Unbalanced-Mass Devices for Scanning Gimbaled Payloads and Free-Flying Spacecraft

(CDDF Final Report No. 92–02)

D.C. Alhorn and M.E. Polites

George C. Marshall Space Flight Center

Marshall Space Flight Center, Alabama

National Aeronautics and Space Administration

Office of Management

Scientific and Technical Information Program

TABLE OF CONTENTS

LIST OF ILLUSTRATIONS

LIST OF ILLUSTRATIONS (Continue)

LIST OF TABLES

TECHNICAL PAPER

RESULTS OF A LABORATORY EXPERIMENT THAT TESTS ROTATING UNBALANCED-MASS DEVICES FOR SCANNING GIMBALED PAYLOADS AND FREE-FLYING SPACECRAFT

(MSFC Center Director's Discretionary Fund Final Report, Project Number 92–02)

I. INTRODUCTION

Space-based and balloon-borne gimbaled scientific instruments often require scanning to meet their scientific objectives. The same is true of some free-flying spacecraft. See references 1 to 3 for examples of these. Sometimes, the only possible way to achieve a meaningful scan is to scan the entire instrument or spacecraft. This is true for x-ray and gamma-ray telescopes. The scan patterns required are often linear scans, raster scans, or circular scans. A linear scan is characterized by the instrument or payload line-of-sight repeatedly moving back-and-forth in a line centered on the target. A raster scan is like a linear scan except with some slow complementary motion in a direction perpendicular to the scanning motion. The complementary motion could be a ramp, a saw-toothed waveform, or stepping motion. Circular scans are characterized by the payload line-of-sight repeatedly tracing out a circle centered on a target.

Gimbaled payloads mounted to space platforms, like the space shuttle or a space station, can be scanned using gimbal-mounted torque motors. However, this approach requires a great deal of power when the payload is large and the scan frequency is high, because the torque motors must continuously accelerate and decelerate the payload very rapidly. Also, this generates large cyclic reaction torques on the mounting base that can excite local structural resonances, causing scanning or stability problems. To help the stability problem, the mounting base would need to be stiffened, which could add considerable mass to the base. In addition, scanning at high frequencies with some precision can require high gimbal servo bandwidths, which may also be difficult to achieve. A large payload inertia and mass, interacting with any structural flexibility in the gimbals or the torque motors, can produce low-frequency structural resonances which severely limit the servo bandwidth that is attainable with a stable control system. Scanning large payloads at high frequencies means large gimbal torque motors, which have more cogging, ripple, and friction than small ones. With a digital implementation for the gimbal servos, the torque commands to large torque motors have more quantization than those to small torque motors. All of these problems can degrade scanning accuracy. Using control moment gyroscopes (CMG's) or reaction wheels, in place of gimbal torque motors, does not require torquing against the mounting base, but does not eliminate the other problems.

The problems with scanning balloon-borne gimbaled payloads using torque motors, CMG's, or reaction wheels are worse than those just described. Now the gimbaled payload is mounted to a gondola, which has much less mass than the space shuttle or a space station. In fact, it may have less mass than the payload being scanned. What is worse, the gondola attaches to a set of shroud lines, which in turn attaches to a balloon. Therefore, the plant dynamics are extremely complex, which exacerbates the scanning problems.

Obviously, free-flying spacecraft cannot be scanned with gimbal torque motors; but they can be scanned with CMG's or reaction wheels. The plant dynamics of a free-flying spacecraft are more benign than those of a balloon-borne gimbaled payload, but the other problems with scanning a large payload at high frequencies are just as bad.

References 4 through 7 describe a new approach to scanning space-based and balloon-borne gimbaled payloads, free-flying spacecraft, as well as ground-based gimbaled payloads. It uses a pair of rotating unbalanced-mass (RUM) devices, mounted on the payload or spacecraft, to generate the basic scan motion and an auxiliary control system (ACS) which: (1) keeps the scan centered on the target and (2) produces a complementary motion for raster scanning. The ACS can use gimbal torque motors, CMG's, or reaction wheels, depending on the application, but is not required to have a high bandwidth. Rather, it only has to generate low-frequency, low-amplitude torques to satisfy its requirements. Thus, large cyclic reaction torques against a mounting base or gondola are avoided when RUM's are used for scanning. The analysis and computer simulation results in references 4 and 5 show that gimbaled payloads and free-flying spacecraft can scan more accurately and with much less power when RUM's are used. However, these claims have never been proven by actual hardware testing, until now.

This paper describes an actual laboratory experiment that tests the concept of scanning a gimbaled payload with RUM devices. Test results from the experiment are presented, which prove the concept. The outline of the paper is as follows. Section II presents the basic theory of scanning with RUM devices. Section III describes in detail the laboratory experiment for testing RUM's. Section IV covers the procedures used in testing. Section V presents the test results for linear scanning, with and without RUM's, and compares these with results from a computer simulation model. Section VI is similar to section V, except for circular scanning. Section VII offers conclusions and final comments.

II. THE BASIC THEORY OF SCANNING WITH RUM DEVICES

The basic concept of a RUM device can be explained with the help of figures 1 and 2, which show a gimbaled I-beam as an emulated payload to be scanned. A pair of RUM's is mounted on top of the I-beam for linear scanning in cross-elevation. Another pair is mounted on the lower side for circular scanning.

A RUM device is simply a mass, m, on a lever arm, r, rotating at a constant angular velocity,

$$\omega = \frac{2\pi}{T_P} \quad , \tag{1}$$

where T_P is the period of rotation of the mass. This generates a centrifugal force, $m\omega^2 r$, on the payload. Mounting the RUM device at a distance, d, from payload center-of-mass generates a cyclic torque, about the center-of-mass, with an amplitude equal to $m\omega^2 rd$.

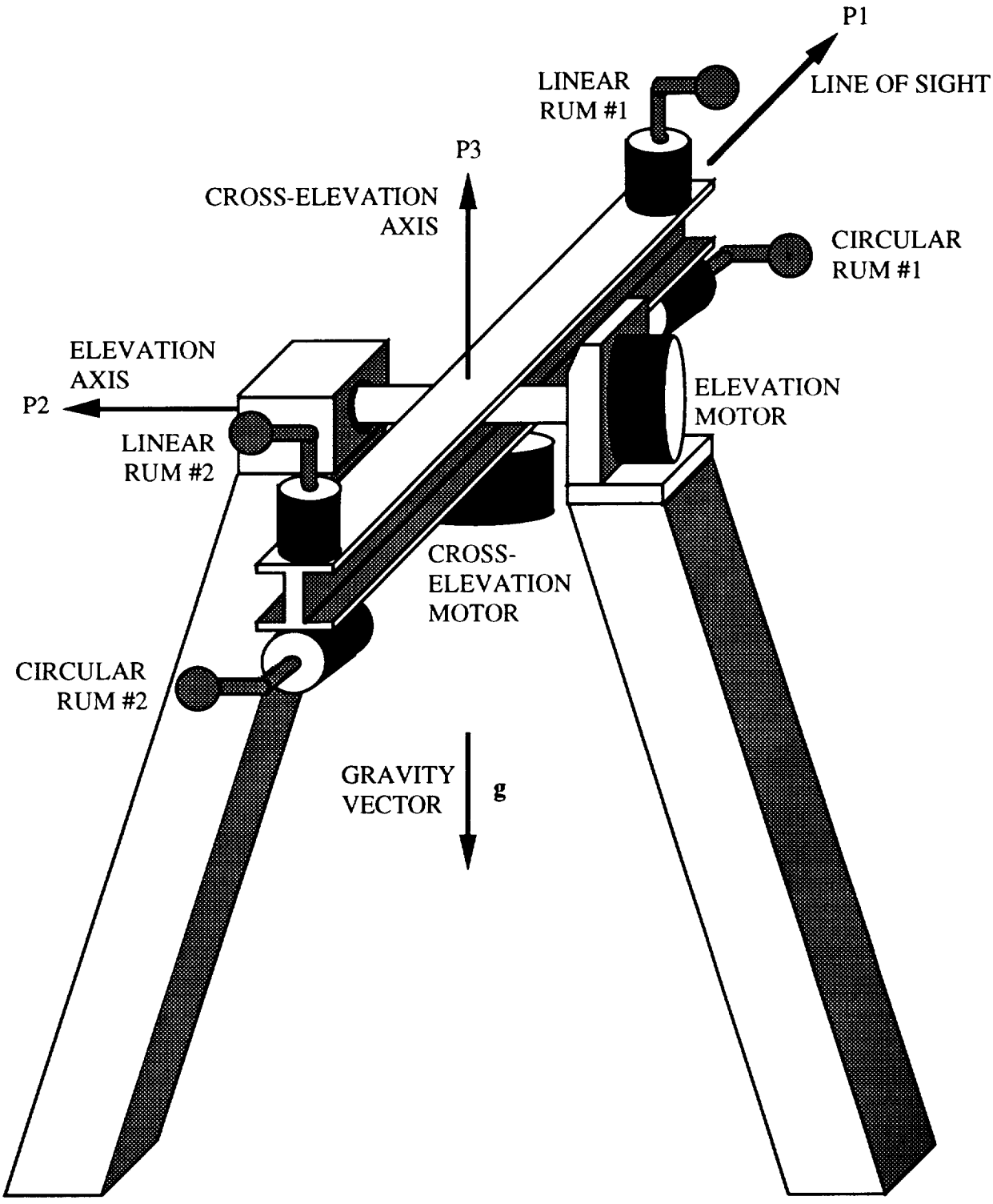

Figure 1. Concept of an experiment to test RUM devices for linear, raster, and circular scanning.

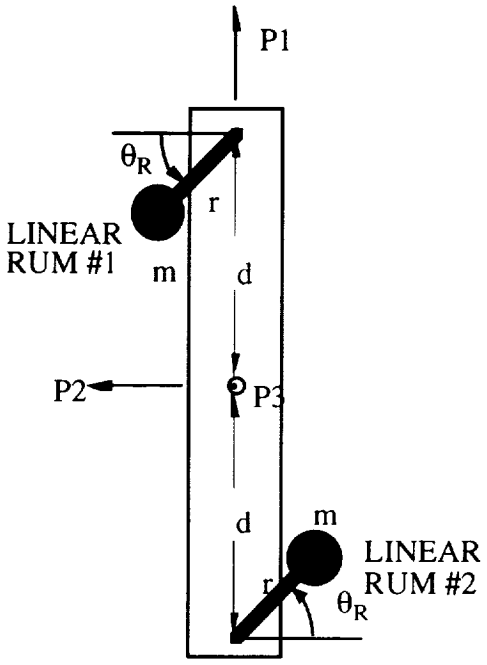

(a)
View looking down P3 axis showing linear RUM parameters.

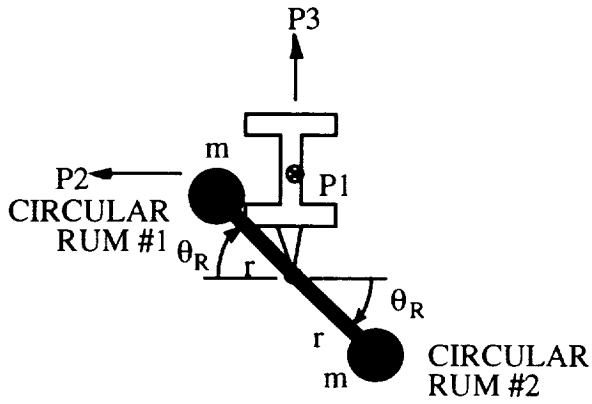

(b)
View looking along P1 axis showing circular RUM parameters.

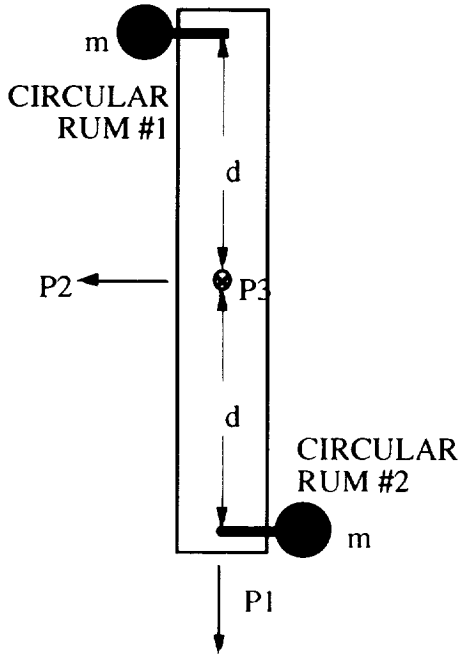

(c)
View looking along P3 axis showing circular RUM parameters.

Figure 2. Definition of the RUM parameters.

When the top RUM's in figure 1 are maintained 180° out-of-phase as they rotate about the cross-elevation axis (P3), the net torque is cyclic in the cross-elevation axis and has a magnitude of $2m\omega^2 rd$. When the RUM positions are defined by the angle Θ_R in figure 2-a and

$$\Theta_R = \omega t = \frac{2\pi}{T_P} t \ , \tag{2}$$

then the net torque in cross-elevation becomes

$$T_X = 2m\omega^2 rd\cos(\Theta_R) = 2m\omega^2 rd\cos\left[\frac{2\pi}{T_P} t\right] \ . \tag{3}$$

Using the definitions for the payload cross-elevation angle Θ_X and elevation angle Θ_E shown in figure 3, the payload equation-of-motion in cross-elevation can be approximated by

$$\ddot{\Theta}_X = \frac{T_X}{I} \ , \tag{4}$$

where I is the payload moment-of-inertia in the cross-elevation axis. Equation (4) neglects any friction in the system and assumes perfect cancellation of the reaction torques on the payload caused by any

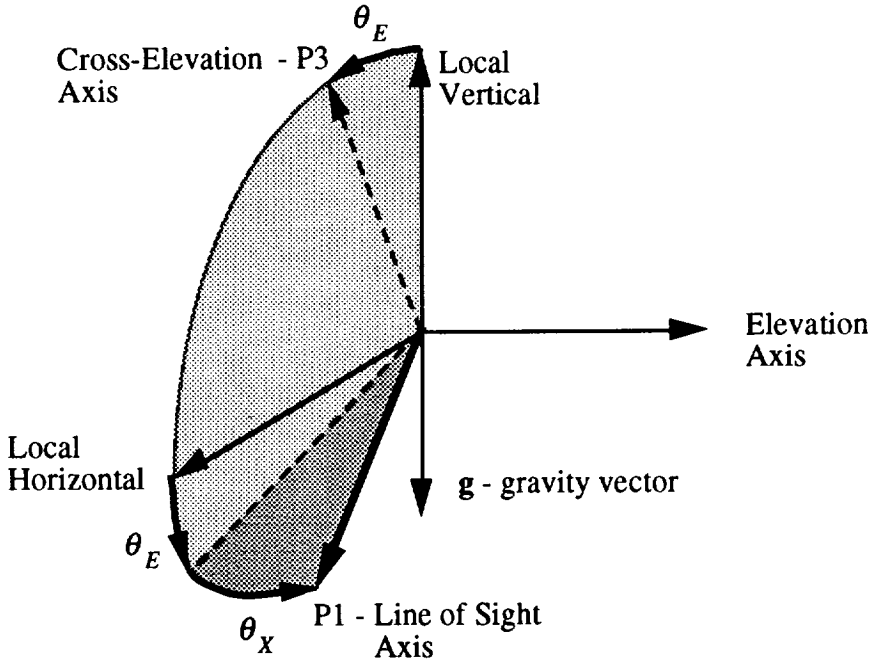

Figure 3. Definition of the elevation and cross-elevation gimbal angles.

gravity torques on the RUM masses. Substituting equation (3) into equation (4) and integrating twice gives the steady-state scan motion:

$$\Theta_X = -\frac{2mrd}{I}\cos\left[\frac{2\pi}{T_P}t\right] = -\rho\cos\left[\frac{2\pi}{T_P}t\right] . \tag{5}$$

As expected, this represents linear scan motion in the cross-elevation axis with an amplitude

$$\rho = \frac{2mrd}{I} \tag{6}$$

and a period T_P, the same as the period of rotation of the RUM's. Hence, changing the lever arm of the RUM devices is a convenient way to change the scan amplitude. Similarly, a simple way to change the scan period is to change the RUM period of rotation, since both are equal to T_P.

When the lower RUM's in figure 1 are maintained 180° out-of-phase as they rotate about the payload line-of-sight (P1), the net torque is now cyclic in both the cross-elevation and elevation axes and has a magnitude of $2m\omega^2 rd$. When the RUM positions are specified by the angle Θ_R in figure 2-b and Θ_R as a function of time is defined by equation (2), then the net torques in the cross-elevation and elevation axes are, respectively,

$$T_X = +2m\omega^2 rd\cos(\Theta_R) = +2m\omega^2 rd\cos\left[\frac{2\pi}{T_P}t\right] \tag{7}$$

$$T_E = -2m\omega^2 rd\sin(\Theta_R) = -2m\omega^2 rd\sin\left[\frac{2\pi}{T_P}t\right] . \tag{8}$$

Using the definitions for the payload cross-elevation angle Θ_X and elevation angle Θ_E shown in figure 3, the payload equations-of-motion in cross-elevation and elevation can now be approximated by

$$\ddot{\Theta}_X = \frac{T_X}{I} \tag{9}$$

$$\ddot{\Theta}_E = \frac{T_E}{I} \tag{10}$$

respectively, when I is the payload moment-of-inertia in both the cross-elevation and the elevation axes. Again, equations (9) and (10) neglect any friction in the system and assume exact cancellation of the reaction torques on the payload caused by any gravity torques on the RUM masses. Substituting equations (7) and (8) into equations (9) and (10), respectively, and integrating twice gives the steady-state scan motion

$$\Theta_X = -\frac{2mrd}{I}\cos\left[\frac{2\pi}{T_P}t\right] = -\rho\cos\left[\frac{2\pi}{T_P}t\right] \tag{11}$$

$$\Theta_E = +\frac{2mrd}{I}\sin\left[\frac{2\pi}{T_P}t\right] = +\rho\sin\left[\frac{2\pi}{T_P}t\right] \quad . \tag{12}$$

Clearly, this is circular motion of the payload line-of-sight. The scan radius is ρ and specified by equation (6); the scan period is T_P, the same as the RUM's period of rotation. Like before, changing the lever arm of the RUM devices is a convenient way to change the scan radius and changing the RUM's period of rotation changes the scan period.

With either linear or circular scanning, the RUM's are required to rotate at a constant angular velocity and stay 180° out-of-phase with each other. To achieve this, each RUM device requires a servo with a torque motor and an angular position sensor, like an optical encoder. If the scan rates are not too high, the feedback controller for both servos can be implemented digitally in a single microcontroller; otherwise, analog electronics are recommended. Other implementations for the RUM servos are possible. For example, resolvers can be used in place of encoders; and tachometers could be added for rate feedback.

To keep the RUM-generated scan on target and produce the complementary motion for raster scanning, the ACS is needed. The commands to the ACS need to be synchronized with the motion of the RUM's, so that the ACS does not fight the scan motion generated by the RUM's. For the gimbaled I-beam in figure 1, the ACS employs the gimbal torque motors.

The choice of the payload sensors depends on the target to be scanned and the application. For example, if the payload scans the Sun, a payload-mounted two-axis Sun sensor is recommended. A payload mounted two-axis rate gyro can be added for rate feedback. To simply demonstrate the concept of scanning with RUM devices, gimbal encoders or resolvers are sufficient for position information and gimbal-mounted tachometers can be added for rate feedback. If the RUM servos have a microcontroller, it can also be used to solve the control algorithms for the ACS.

III. THE EXPERIMENT FOR TESTING RUM DEVICES

Initially, an experiment was conceived to test a pair of RUM devices for linear and raster scanning a gimbaled payload. A detailed design was performed and a computer simulation model was developed to verify the design. This is documented in reference 8. Then, modifications to the experiment were defined in order to reconfigure it for circular scanning. The computer simulation model was also modified and used to verify the experiment design for circular scanning. See reference 9 for further information.

Subsequently, it became apparent that the experiment could not be quickly reconfigured for one type of scanning or another, using only one pair of RUM's. This is because the RUM's have to be reoriented to change scans and the payload has to be rebalanced to keep its center-of-mass at the intersection of the cross-elevation and the elevation gimbals. To circumvent this problem, two pairs of RUM's were used in the final experiment, as shown in figure 1 and in the actual experiment in figures 4 and 5. The top pair of RUM devices was used for linear and raster scanning and the lower pair was used for circular scanning. In this experiment, only one pair of RUM devices was operated at a time and the other pair was mechanically locked and powered down. Figure 6 is a close-up of two separate RUM devices on one end of the payload.

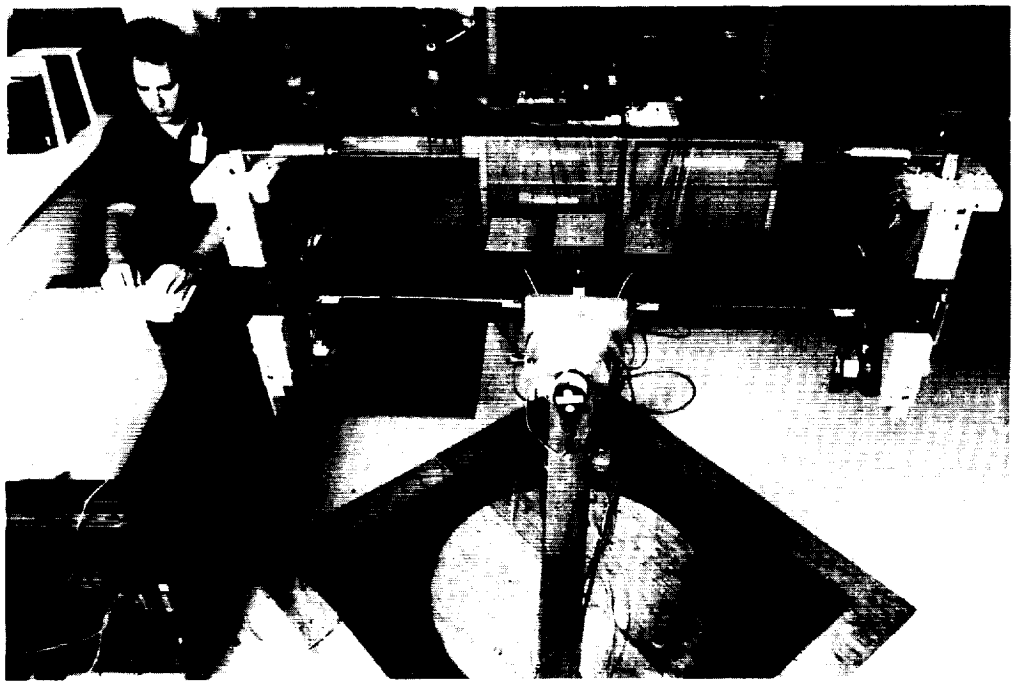

Figure 4. Photograph of the completed RUM experiment.

Figure 5. Dean Alhorn at the host computer and Mike Polites at the emulated payload.

Figure 6. A close-up of two RUM devices mounted on one end of the payload.

In figures 4 and 5, the control electronics for the servos in the experiment are located on the lab bench in the background. The host computer in the photographs was used to program the microcontroller, which performs the control algorithm computations for the RUM and gimbal servos. In addition, the host computer served several other purposes. It was used to initialize the experiment for scanning; it provided a means to change parameters in the system, like the scan period; and, it was used to retrieve data periodically from the microcontroller and store it on disk. Later, this data was analyzed and plotted to show the performance of the various scans.

In figures 4 through 6, each RUM has a mass m = 5 lb = 0.155 slugs, on a lever arm r = 0.5 ft, located at a distance d = 2.5 ft from the payload center-of-mass. Mounted on the rotational axis of each RUM device is: a direct-drive brushless DC torque motor with a motor constant K_{MR} = 0.57 ft-lb/$\sqrt{W}$; and an incremental optical encoder, with a resolution of 1.8 arc-min, used to determine the RUM angle.

The payload is a 170 lb, 5 ft long steel I-beam with a 6-in by 6-in cross-section and a flange width of 0.5 in. Including the RUM devices and mounting fixtures, the total payload mass is about 250 lb. When the payload was circular scanned for a short period of time using only the RUM's, the amplitude of the scan was observed to be about ρ = 51 arc-min = 0.0149 rad. Using equation (6) and the other known parameters, the moments-of-inertia in cross-elevation and elevation were computed to be about I = 26 slug-ft^2.

The gimbals supporting the payload have a freedom of ±15° in cross-elevation and ±90° in elevation, using the conventions for the cross-elevation angle Θ_X and elevation angle Θ_E shown in figure 3. On each gimbal axis is: a direct-drive DC torque motor with ± 11 ft-lb peak torque, a motor constant K_{MG} = 0.61 ft-lb/$\sqrt{W}$, and a 4 percent ripple torque; an incremental encoder, identical to the ones in the RUM's, for measuring gimbal position; and a tachometer, with 0.48 V/rad/sec sensitivity and 1 percent ripple voltage, to measure the gimbal rate.

All RUM and gimbal servos are controlled by an INTEL 80C196KC microcontroller. It samples all sensor outputs, solves the control algorithms, and issues torque motor commands every T = 7.5 milliseconds. A control system block diagram for the RUM servos is shown in figure 7. Effectively, this is a rate servo with a control law that has proportional, integral, and double integral terms. The control law parameters were selected for a 10 Hz servo bandwidth. The computed torque commands are quantized by 12 bit D/A converters, which are scaled for an LSB of 0.0085 ft-lb. These are issued every computation cycle to the power amplifiers that drive the RUM torque motors. Prior to scanning, the two RUM's being utilized are positioned so the RUM angle, defined by either figure 2-a or 2-b, is Θ_R = 0°. This properly initializes them to be 180° out-of-phase. Once scanning begins, the RUM servos automatically maintain this relationship, when the same commanded change in RUM angle, $\Delta\theta_{RC}$, is issued to each servo every computation cycle. The magnitude of this command determines the period-of-rotation T_P for the RUM's. When $\Delta\theta_{RC}$ is expressed in rad, the governing relationship is:

$$\Delta\theta_{RC} = 2\pi\frac{T}{T_P} \quad . \tag{13}$$

The control system block diagrams for the cross-elevation and the elevation servos are shown in figures 8 and 9, respectively. For each gimbal servo, the microcontroller reads the incremental encoder output every computation cycle (i.e. every T = 7.5 millisec) and sums these to generate an estimate of the gimbal angle. Each tachometer output is filtered by an analog low-pass filter that rolls off at 46 Hz.

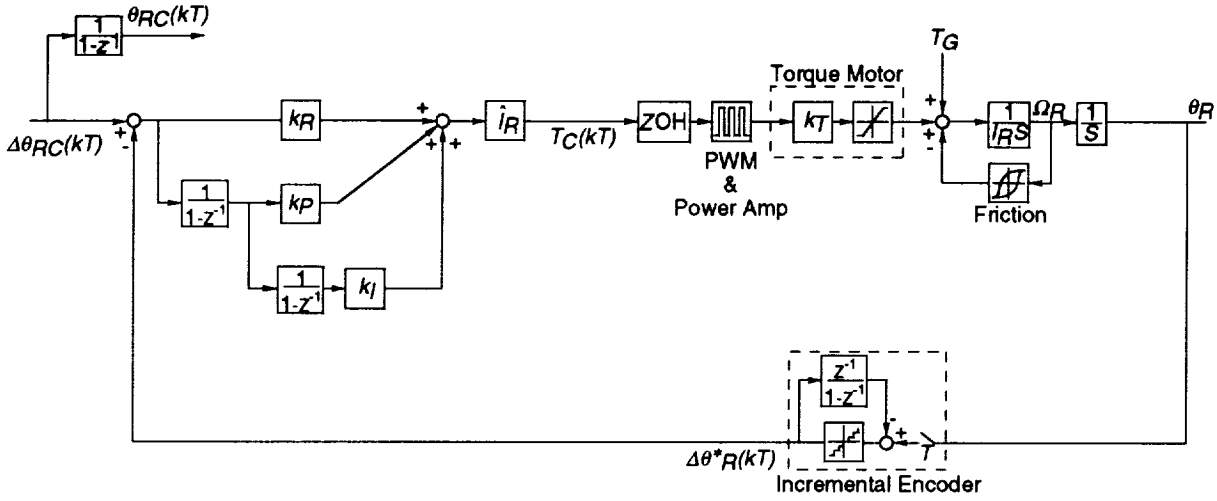

Figure 7. Control system block diagram for the RUM servos.

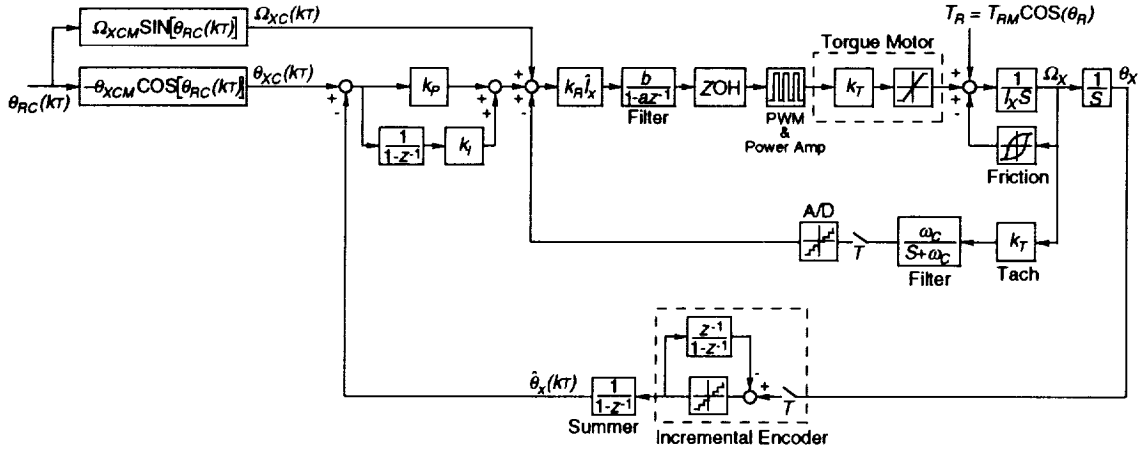

Figure 8. Control system block diagram for the cross-elevation servo.

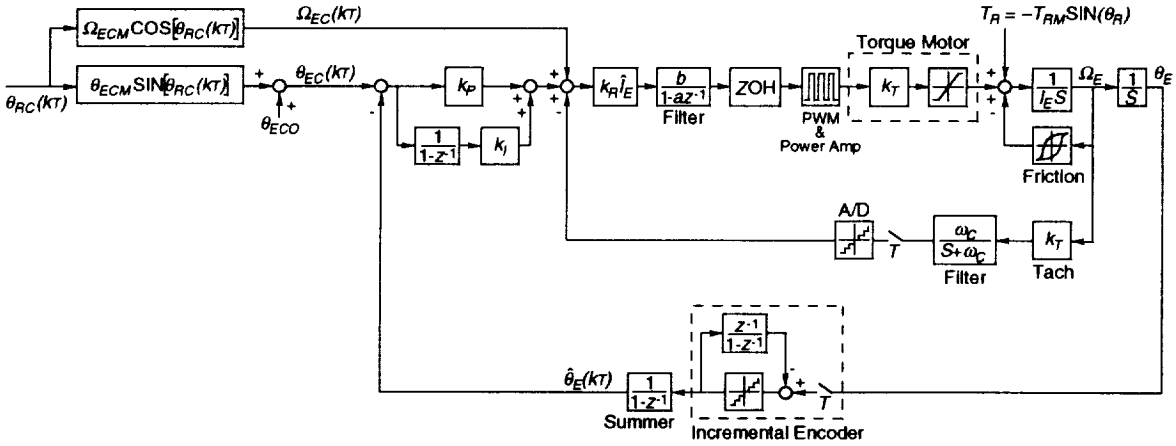

Figure 9. Control system block diagram for the elevation servo.

The filter output is sampled every computation cycle by a 10 bit A/D converter scaled to a range of ±0.35 rad/sec or ±20°/sec. This gives an LSB of about 0.04°/sec. Gimbal angle and rate commands are computed in the microcontroller every computation cycle. These are synchronized with the RUM motion so the RUM's and the gimbal servos work together synergistically. This is accomplished by summing the commanded changes in the RUM angle, $\Delta\theta_{RC}$, each computation cycle, in order to generate the commanded RUM angle θ_{RC}. This is shown in figure 7. Then, θ_{RC} is input into the computations for the gimbal angle and rate commands shown in figures 8 and 9. When only the gimbal servos are used for scanning, the operation is the same except that all four RUM's are mechanically locked and powered down.

For circular scanning, the constants θ_{XCM} and θ_{ECM} were determined to be:

$$\theta_{XCM} = \theta_{ECM} = \rho = 51 \text{ arc-min} = 0.0149 \text{ rad.} \tag{14}$$

Here, ρ was determined by observing the natural scan radius when the RUM's were activated for a short period of time without the gimbal servos. An alternative is to compute ρ using equation (6), provided the system parameters are accurately known . The constants Ω_{XCM} and Ω_{ECM} were determined to be:

$$\Omega_{XCM} = \Omega_{ECM} = \frac{2\pi}{T_P}\rho = 322 \text{ arc-min/sec} = 5.37°/\text{sec} = 0.0937 \text{ rad/sec} \ , \tag{15}$$

when the scan period T_P = 1 sec, which was the baseline for all tests.

For linear scanning, the only difference is

$$\theta_{ECM} = \Omega_{ECM} = 0. \tag{16}$$

In figure 9, specifying the bias elevation angle command θ_{ECO} determines the nominal elevation angle for circular or linear scanning. Varying θ_{ECO} as a function of time generates the complementary motion for raster scanning.

The control law for each gimbal servo is a proportional-integral controller with rate feedback. The control gains were chosen for a servo bandwidth of approximately 0.1 Hz. In fact, structural resonances in the system made it impossible to get a higher bandwidth and still have a stable control system. In the forward loop of each servo is a digital low-pass filter that rolls off at 2 Hz. It prevents exciting these structural resonances as much as possible. The output of the digital filter is the torque command for the gimbal torque motor. Its magnitude is quantized to 8 bits, with each bit corresponding to about 0.05 ft-lb. The quantized torque command is issued by the microcontroller every computation cycle to a PWM generator, which in turn drives the power amplifier for the gimbal torque motor.

IV. PROCEDURES FOR TESTING THE RUM DEVICES

Prior to testing the RUM's for scanning, the payload with all four RUM's was roughly mass balanced. This was accomplished by first locking the RUM's in place and then driving the elevation servo to a -90° elevation angle. The steady state torque command in the elevation servo was then

observed using the host computer. With this information, the mass needed to balance the I-beam was determined. Then, steel plates with this mass were mounted on the I-beam, as shown in figures 4 and 5. This reduced the elevation torque command to less than 1 ft-lb, which is small compared to the 11 ft-lb peak torque of the elevation torque motor.

To test the RUM devices for scanning the payload, a number of scans were performed. Linear and circular scans were generated, with and without RUM devices, at nominal elevation angles of 0 and –90°. A 0° elevation angle is the best orientation for linear scanning with RUM's, because no gravity torque acts on them. Therefore, this is like a simulated zero-g test for linear scanning with RUM's. A –90° elevation angle is the worst orientation for linear scanning with RUM's, because the gravity torque acting on them is a maximum. Just the opposite is true for circular scanning with RUM's. As a result, these two elevation angles cover both extremes for both types of scanning with RUM's. Scanning without RUM's should give similar results at any elevation angle, when the payload is properly mass balanced. Raster scanning to test RUM devices has one drawback. The entire system never truly reaches steady state, because the peak gravity torque on the RUM's continually changes with the changing elevation angle. For this reason, linear and circular scans were used to evaluate scanning with and without RUM's. Raster scanning was observed and verified, but no results are included here.

For a given scan, about 2 minutes was allowed for the system to reach steady state. Then, over the next 15 sec, the gimbal and RUM servo variables were sent every computation cycle (i.e. every 7.5 milliseconds) from the microcontroller to the host computer and stored on disk. Later, this data was prepared for plotting. The important criteria for judging the results of scanning, with and without RUM's, are the size of the scan, the scan errors, the torques generated by the torque motors used in the scan, and the power dissipated in these torque motors. For each scan, these performance criteria were determined from the variables sent to the host computer.

The size of the scan was determined from the measured cross-elevation and elevation gimbal angles used in the gimbal servos. These values were obtained by summing the gimbal incremental-encoder outputs in the microcontroller. When the nominal elevation angle was –90°, then –90° was first subtracted from the stored values for the elevation angles before plotting, in order to give better plot resolution. Then, the gimbal angles were plotted versus time, in the case of a linear scan. They were plotted versus each other, in the case of a circular scan.

The scan errors were determined from the gimbal angle errors in the gimbal servos. These were arrived at by differencing the gimbal angle commands with the measured gimbal angles. The elevation errors were not altered before plotting and both errors were plotted versus time for both linear and circular scanning. In addition, the RMS values of these errors, over the 15 sec intervals, were computed and tabulated, in all cases.

The RUM experiment was not designed to directly measure the torque, current, or power of any motor; so, an indirect method was used to estimate the torque and power of each motor during scanning. This method utilized the torque motor commands in both the gimbal and RUM servos. The torque motor command data was multiplied by an appropriate scale factor that relates the commands to the delivered torque for each motor in order to estimate the actual motor torques. For the RUM torque motors, these scale factors were determined by holding the I-beam fixed, using the gimbal servos, and positioning the RUM masses for a maximum gravity torque (2.5 ft-lb), using the RUM servos. Dividing 2.5 ft-lb by the steady state torque commands in the RUM servos gave the scale factor 0.90 for the RUM torque motors. For the gimbal torque motors, these scale factors were determined by holding the I-beam fixed using the gimbal servos and positioning the RUM's so they were 180° out-of-phase and contributed no imbalance

torque to the I-beam. One RUM was then rotated 180° to produce a known change to the imbalance torque on the I-beam (5 ft-lb). Dividing this torque by the observed change in the torque command for the appropriate gimbal servo, gave the scale factor 0.78 for both gimbal motors. The estimated motor torques were plotted versus time in all cases.

Next, the RMS values for the estimated RUM motor torques, $T_{R1(RMS)}$ and $T_{R2(RMS)}$, were computed over each 15 sec interval. The estimated RMS power dissipated in the RUM motors was computed as follows:

$$P_{R(RMS)} = \left[\frac{T_{R1(RMS)}}{K_{MR}}\right]^2 + \left[\frac{T_{R2(RMS)}}{K_{MR}}\right]^2 \quad (17)$$

where $K_{MR} = 0.57$ ft-lb/$\sqrt{W}$.

A similar, but slightly different procedure was used for the gimbal motors. Here, the mean and the standard deviation of the estimated gimbal motor torques were computed over each 15 sec interval. Denoting the standard deviations by $T_{X(SD)}$ and $T_{E(SD)}$, the estimated RMS power dissipated in the gimbal motors was computed from the relationship:

$$P_{G(RMS)} = \left[\frac{T_{X(SD)}}{K_{MG}}\right]^2 + \left[\frac{T_{E(SD)}}{K_{MG}}\right]^2 \quad (18)$$

where $K_{MG} = 0.61$ ft-lb/$\sqrt{W}$. This procedure was used, because better mass balancing of the payload could have eliminated the mean gimbal torques. When the mean is zero, the standard deviation is equal to the RMS. The sum of $P_{R(RMS)}$ and $P_{G(RMS)}$ gave the estimated total RMS power dissipated in all motors used in a given scan. Of course, if the scan is performed without RUM devices, then the RUM motor torques are zero and $P_{R(RMS)} = 0$.

V. TEST RESULTS FOR LINEAR SCANNING

The procedures described in section IV were used to obtain the test results from the RUM experiments which are presented here. Figure 10 shows the actual steady state time responses from the RUM experiment for a linear scan with a 1 sec period, using RUM's and gimbal servos. The scan was performed at a nominal elevation angle of 0°. This payload orientation simulates linear scanning in a zero-g environment.

The data summarizing these results is shown in table 1. A ±51 arc-min scan was generated that is accurate to 1 arc-min RMS in the scan axis. Remember that the measured gimbal angles and gimbal errors are quantized to 1.8 arc-min, which is the resolution of the incremental optical encoders. The total power dissipated in the motors was only 1 watt RMS. For comparison, this same case was run in a simplified computer simulation model of the RUM experiment that was developed from the block

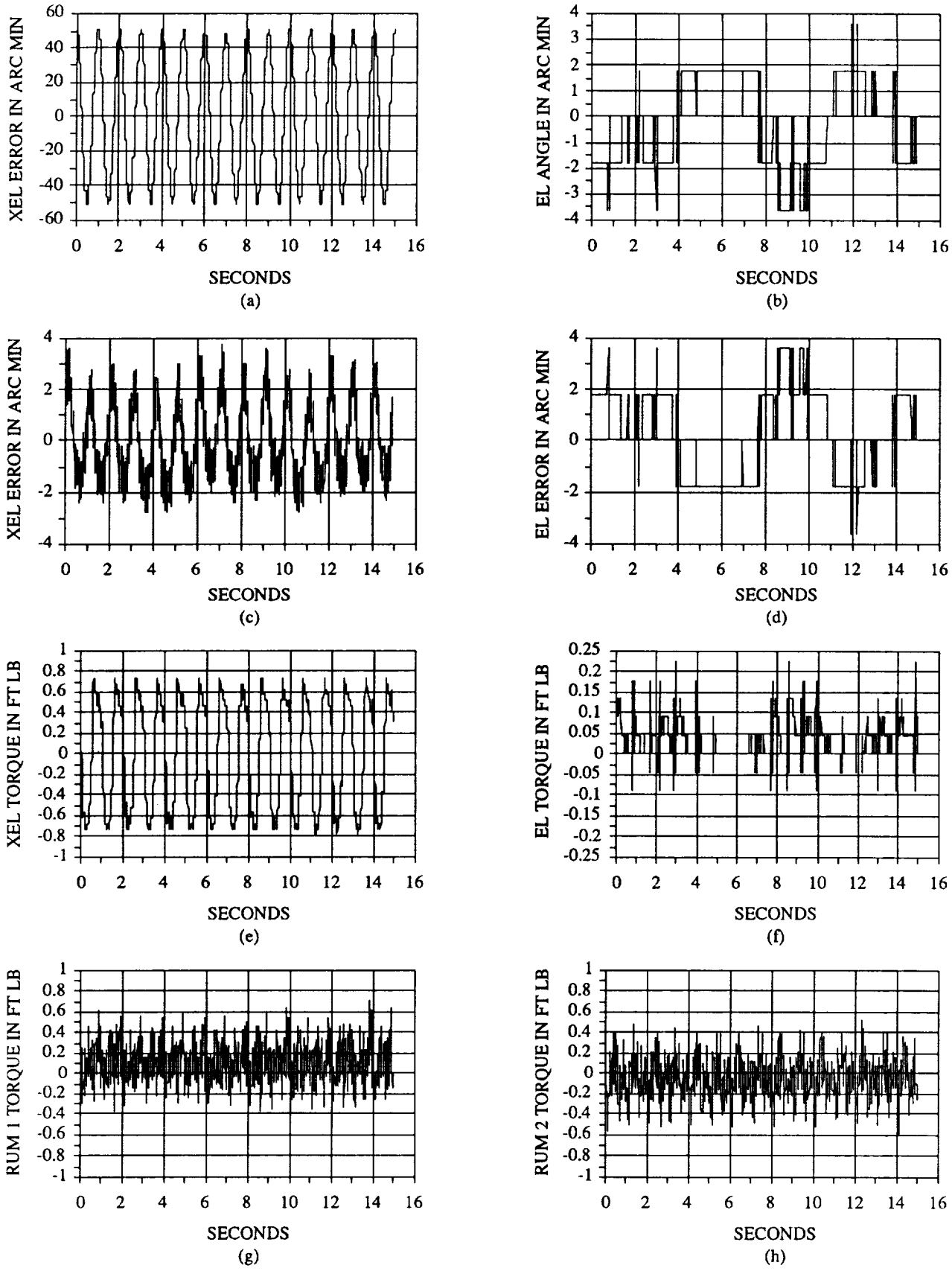

Figure 10. RUM experiment test results for linear scanning with RUM's and gimbal servos at 0° elevation angle.

Table 1. Summary of results from RUM experiment for linear scanning.

EL ANGLE, IN DEG	CMD/ACTUAL SCAN AMPLITUDE, IN ARC-MIN	XEL/EL SCAN ERRORS, IN ARC-MIN RMS[2]	TOTAL POWER FOR TRQ MOTORS USED, IN WATTS RMS[3]
HEADINGS FOR COLUMNS:			
RESULTS USING RUM's AND GIMBAL SERVOS:			
0	51/51[1] (51/51)	1/2 (2/<1)	1 (<1)
-90	51/51 (51/51)	1/1 (2/<1)	29 (21)
RESULTS USING GIMBAL SERVOS ONLY:			
0	51/17 (51/22)	42/2 (42/<1)	79 (49)
0	128/51[4] (128/51)	105/2[4] (105/<1)	494[4] (333)
-90	51/18 (51/22)	42/1 (42/<1)	79 (49)
-90	128/51[4] (128/51)	105/1[4] (105/<1)	494[4] (333)

NOTES:
(1) Top numbers without parentheses are actual hardware results; lower numbers in parentheses are computer simulation results.
(2) Scan errors are error signals in gimbal servos.
(3) Assumes that bias torques of gimbal torque motors can be canceled by better mass balancing.
(4) Extrapolated from result above, based on simulation findings. This is necessary because scan cannot be generated with 11 ft-lb gimbal torque motors that are in RUM experiment.

diagrams shown in figures 7 to 9. The simulation results are also summarized in table 1 by the numbers in parentheses, just under the corresponding values from the RUM experiment. Note that these compare well with the actual test results.

Next, this same scan was attempted using only gimbal servos. The actual test results from the RUM experiment are shown in figure 11, and are also summarized in table 1. The amplitude of the scan decreased to ±17 arc-min, the scan error increased to 42 arc-min RMS in the scan axis, and the total power dissipated in the torque motors increased to 79 watts RMS. These results compared fairly well with those predicted by simulation. The amplitude of the actual scan is 23 percent smaller than that predicted by simulation. The torque motor power is 61 percent larger, which means the RMS torques are about 27 percent larger, since torque is proportional to the square root of power. Thus, the two results match fairly well and the differences are certainly in the right directions, since the computer simulation model is simplified. For example, the simulation assumes no payload products of inertia or mass imbalance, no RUM manufacturing or mounting errors, and a value for gimbal friction that may be optimistic (0.2 ft-lb per axis).

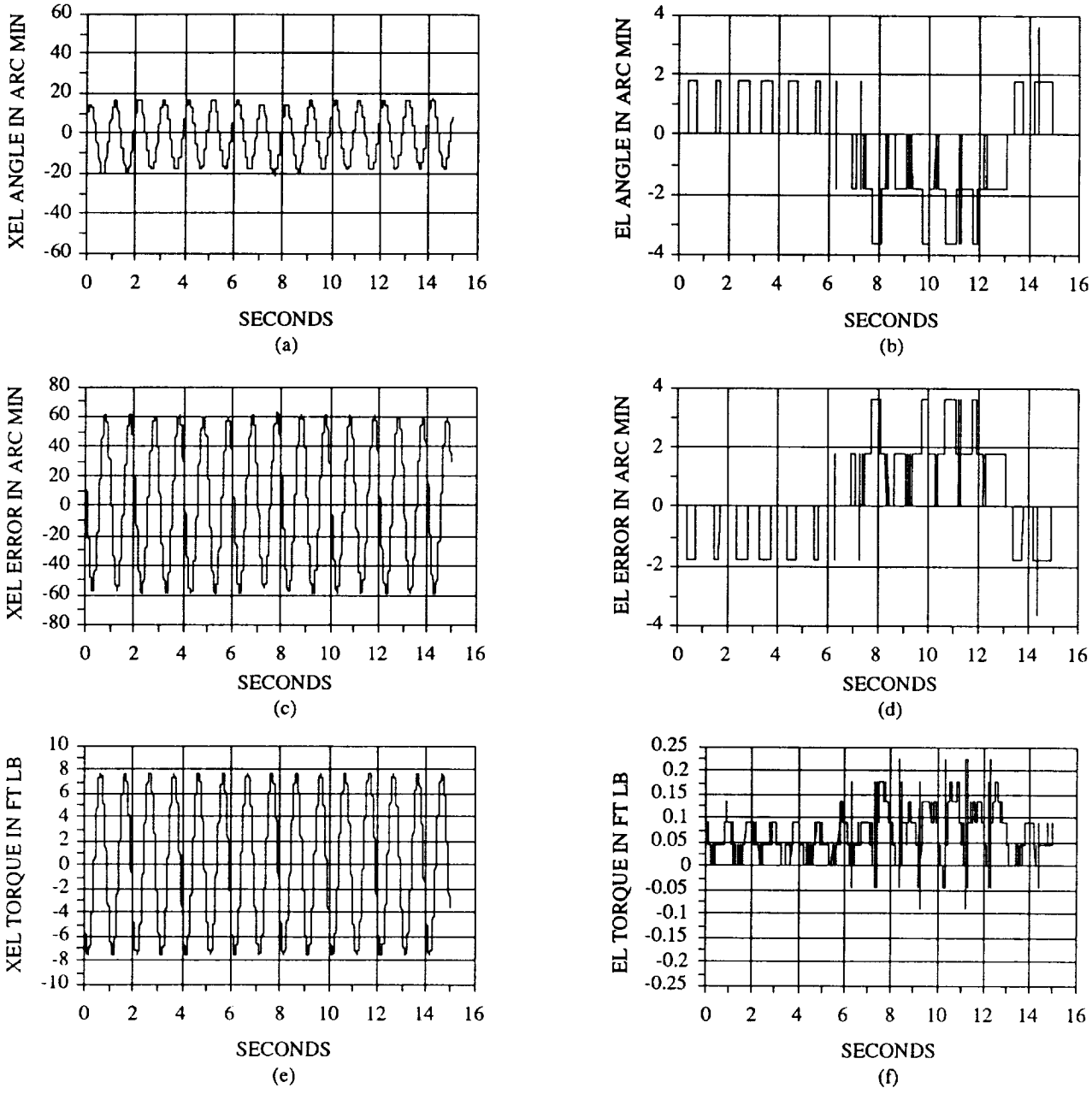

Figure 11. RUM experiment test results for linear scanning with gimbal servos only at 0° elevation angle.

Using only the gimbal servos, a ±51 arc-min scan could be generated, if the amplitude of the commands to them were increased by a factor of 2.5 and the gimbal torque motors were approximately doubled in size, from 11 ft-lb to perhaps 22 ft-lb. Using this approach, the extrapolated test results and the corresponding simulation results are shown in table 1. The extrapolated test results show that when the gimbal servos generate a ± 51 arc-min scan, the scan error is 105 arc-min RMS in the scan axis and the torque motor power is 494 watts RMS.

Therefore, using the RUM's to help generate a ±51 arc-min linear scan at a 0° elevation angle reduces the RMS error in the scan axis by a factor of 105 and reduces the total RMS power dissipated in the torque motors by a factor of 494. The size of the gimbal torque motors can also be reduced, by a factor of 5 or more. Their required peak torque can be reduced from about 22 ft-lb to about 4 ft-lb or less. This means less gimbal motor mass, friction and stiction, cogging and ripple, and better resolution in the torque commands. The reduced mass helps to offset the mass of the RUM devices. The other changes have a positive effect on scan accuracy and power dissipation. Furthermore, the lower reaction torques on the mounting base mean that the base can be less rigid and consequently less massive.

This same methodology was repeated at an elevation angle of –90°. This is the worst orientation for linear scanning with RUM's in one-g, because the gravity torque on them is a maximum. The results at this orientation, scanning with and without RUM's, are shown in figures 12 and 13, respectively, and are again summarized in table 1. At –90°, a ±51 arc-min scan was generated using both the RUM's and gimbal servos. Again the scan accuracy was 1 arc-min RMS in the scan axis and the motor power dissipated in this orientation was now 29 watts RMS.

In this same orientation, a ±51 arc-min linear scan was commanded using only the gimbal servos; however, a ±18 arc-min linear scan was actually generated. The scan accuracy was 42 arc-min RMS in the scan axis and required a total torque motor power of 79 watts RMS. When the gimbal servo commands are increased by a factor of 2.5 and the gimbal torque motors are doubled in size, a ±51 arc-min linear scan can be generated. Except in this case, the scan accuracy is 105 arc-min RMS and the total torque motor power dissipated is 494 watts RMS. These results were derived by extrapolation, as before, and are identical to the extrapolated results at 0° elevation angle, as expected.

Thus, using the RUM's to help generate a ±51 arc-min linear scan at a –90° elevation angle reduces the RMS error in the scan axis by a factor of 105, reduces the total RMS power dissipated in the torque motors by a factor of 17, and allows the size of the gimbal torque motors to be reduced by a factor of 5 or more. The benefits from smaller gimbal motors were previously indicated. Note that these improvements are at a 1 sec scan period.

With lower scan periods, or higher scan frequencies, the improvements are even greater when the RUM's are used for linear scanning. Without the RUM's, each time the scan period is cut in half, the cross-elevation torque motor needs to generate 4 times more torque and dissipate 16 times more power to produce the same sized linear scan. This can be seen by differentiating equation (5) twice, substituting this result into equation (4), and solving for T_X to get

$$T_X = \rho I \left[\frac{2\pi}{T_P}\right]^2 \cos\left[\frac{2\pi}{T_P} t\right]. \tag{19}$$

Therefore, when the scan period T_P is divided by 2, the peak cross-elevation torque increases by a factor of 4. From equations (18) and (19), it becomes apparent that reducing the scan period by a factor of 2 increases the power dissipated in the cross-elevation torque motor by a factor of 16.

On the other hand, when the RUM's are used for scanning, the peak motor torques, and consequently the power dissipated in the motors, are virtually the same at any scan period. This is because the RUM's rotate at a constant angular velocity to generate the scan motion. Furthermore, the

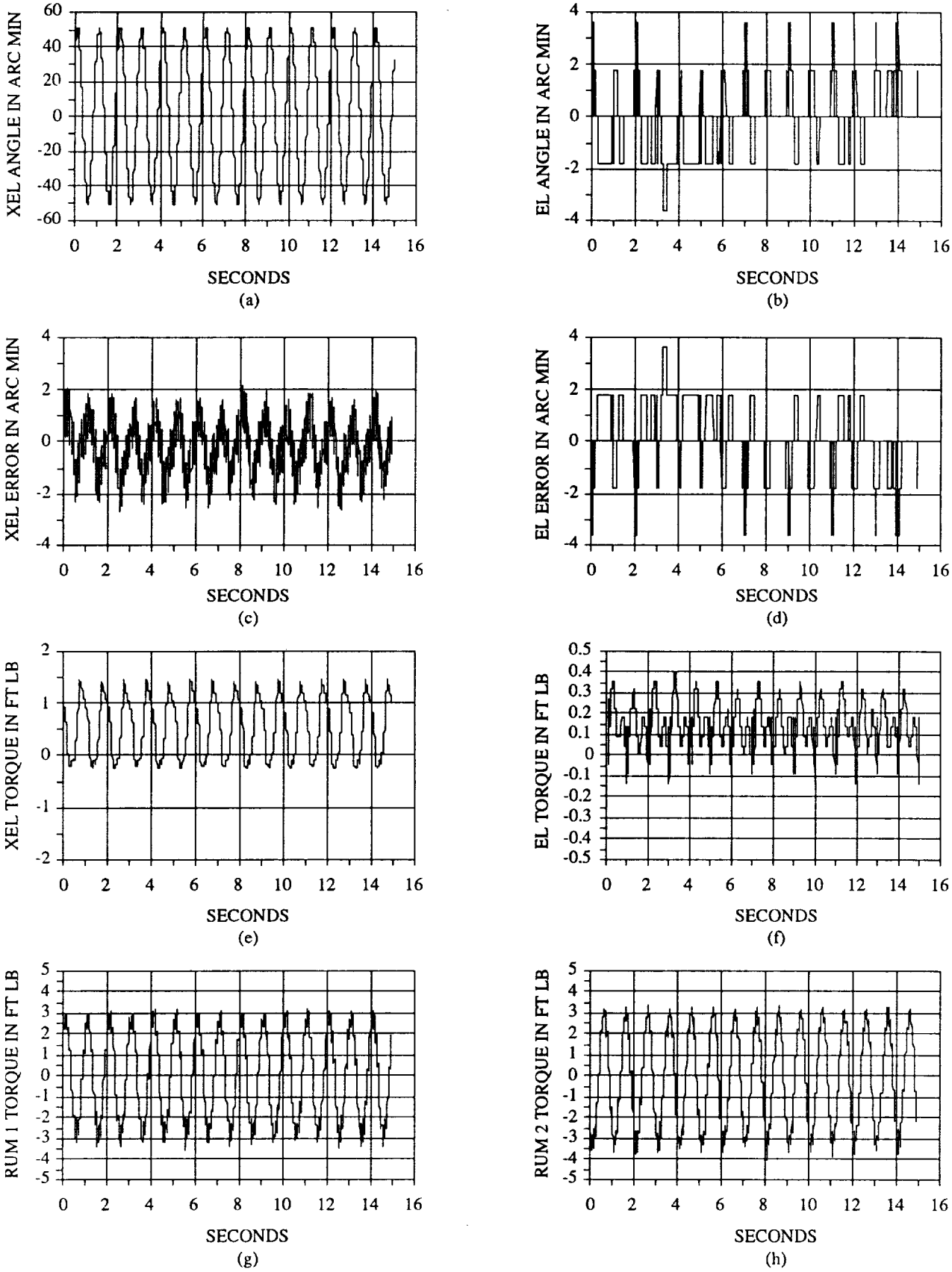

Figure 12. RUM experiment test results for linear scanning with RUM's and gimbal servos at –90° elevation angle.

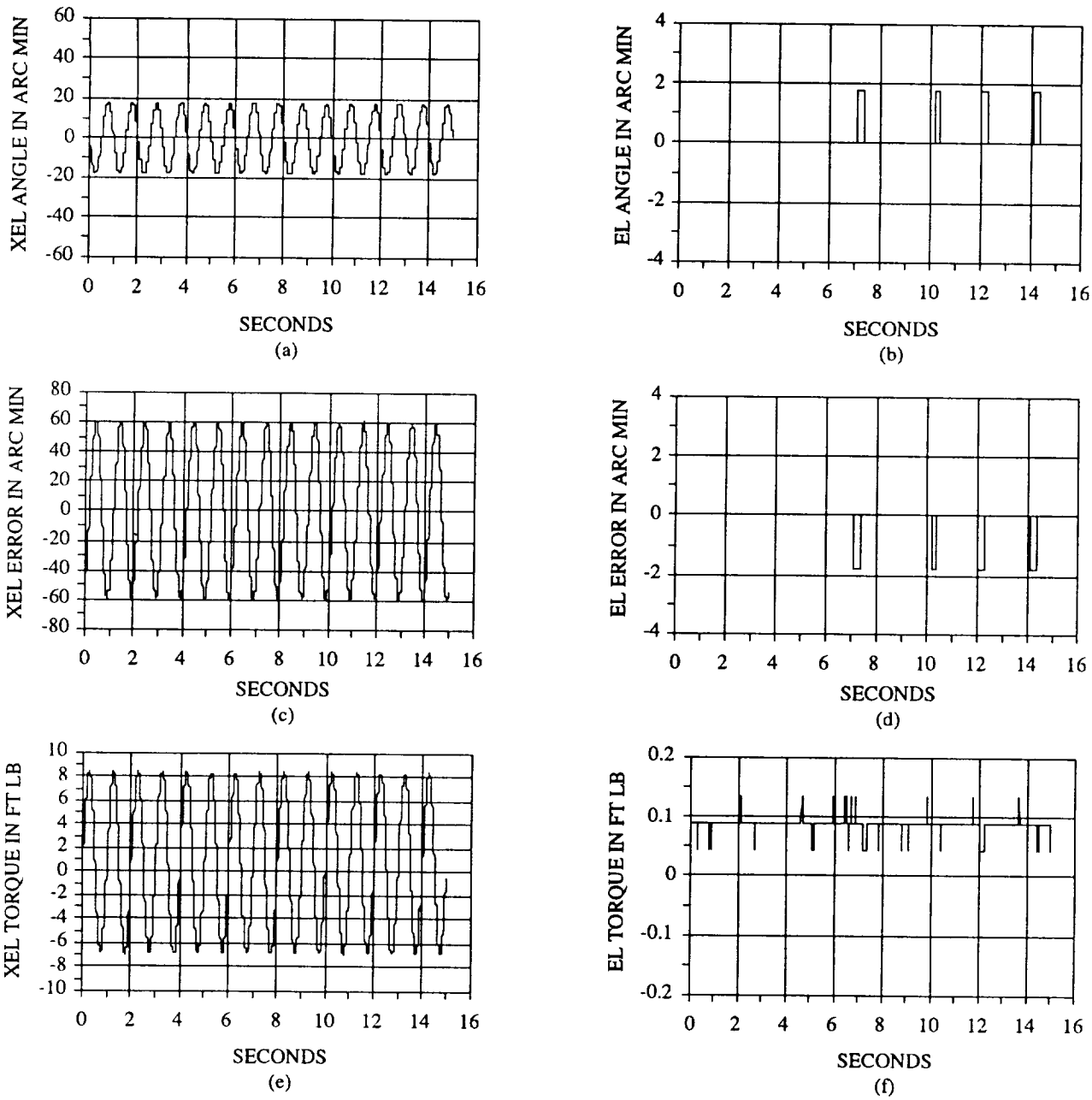

Figure 13. RUM experiment test results for linear scanning with gimbal servos only at –90° elevation angle.

peak gravity torque on the RUM's and the peak friction torques in the RUM devices, gimbal motors and bearings do not change with the scan period. Thus, the power required to scan with the RUM's is essentially independent of the scan period.

It is becoming obvious that scanning large payloads at high frequencies without RUM's can require gimbal motors that are too big and consume too much power to be practical. For example, using gimbal servos only to generate a ±51 arc-min linear scan with a 0.25 sec period requires a

cross-elevation motor with about 350 ft-lb of peak torque. This motor would have to dissipate over 126 kilowatts of RMS power when scanning in either one-g or zero-g. When RUM's are used for the same linear scan, gimbal motors with 4 ft-lb peak torque can be used and the total motor power would be around 29 watts RMS or less in one-g and 1 watt RMS in zero-g.

Also, the amount of motor power required for scanning affects the mass of the electrical system producing this power. To get an idea of this relationship between power and mass for space applications, reference 10 describes the electrical power system for an Earth-orbiting spacecraft. The power generation/storage system delivers about 1 kilowatt of usable power and has a 2,000 lb mass, which includes the solar arrays, batteries and cables. As the power it must deliver goes up, so does its mass. Thus, there is a practical limit to the power that the electrical system can produce for scanning.

VI. TEST RESULTS FOR CIRCULAR SCANNING

The same procedures and methodology used for testing and evaluating linear scanning, with and without RUM's, were used for circular scanning. In this case, a 0° elevation angle is the worst orientation for circular scanning with RUM's in one-g; and a –90° elevation angle is the best orientation and simulates circular scanning with RUM's in zero-g.

Figure 14 shows the actual steady state results from the RUM experiment for circular scanning with the RUM's and gimbal servos. The nominal elevation angle is 0° and the scan period is 1 sec. Instead of plotting the cross-elevation and elevation angles versus time, they were plotted versus each other, to better show the scan pattern generated. The results from figure 14 are summarized in table 2. The results show a 55 arc-min radius circular scan was generated with scan errors of 4 arc-min RMS or less in each axis. The total power dissipated in the four torque motors used for scanning was 32 watts RMS.

For comparison, this same case was run with the computer simulation model of the RUM experiment. These results are shown in figure 15 and are again summarized in table 2 by the numbers in parentheses, just under those from the actual RUM experiment. The two results compare fairly well, since the RMS scan errors were within a factor of 2 of each other. Also, the actual power required by the torque motors was 52 percent more than predicted by simulation, which means the RMS torques are just 23 percent larger. This difference is to be expected, since the computer simulation model is simplified in some respects, as previously indicated.

This same circular scan was attempted in the actual RUM experiment using only gimbal servos. These results are presented in figure 16 and are summarized in table 2. The scan never reaches a steady state condition, because of motion in the elevation axis. The radius of the scan about this motion is approximately 18 arc-min, the scan errors are 42 arc-min RMS or more in each axis, and the power dissipated in the gimbal torque motors is 147 watts RMS. The simulation results for this case are also summarized in table 2 and follow the same pattern previously observed when comparing the simulation results with the actual test results.

Again, if the magnitude of the gimbal servo commands were increased by a factor of 2.5 and the gimbal torque motors were doubled in size, then a circular scan with a 51 arc-min radius could be generated using only the gimbal servos, although its center may still wander. By extrapolation, the predicted results for this case are summarized in table 2. The scan error is now 105 arc-min RMS or more in each axis and the total torque motor power is 919 watts RMS. Therefore, using the RUM's to help

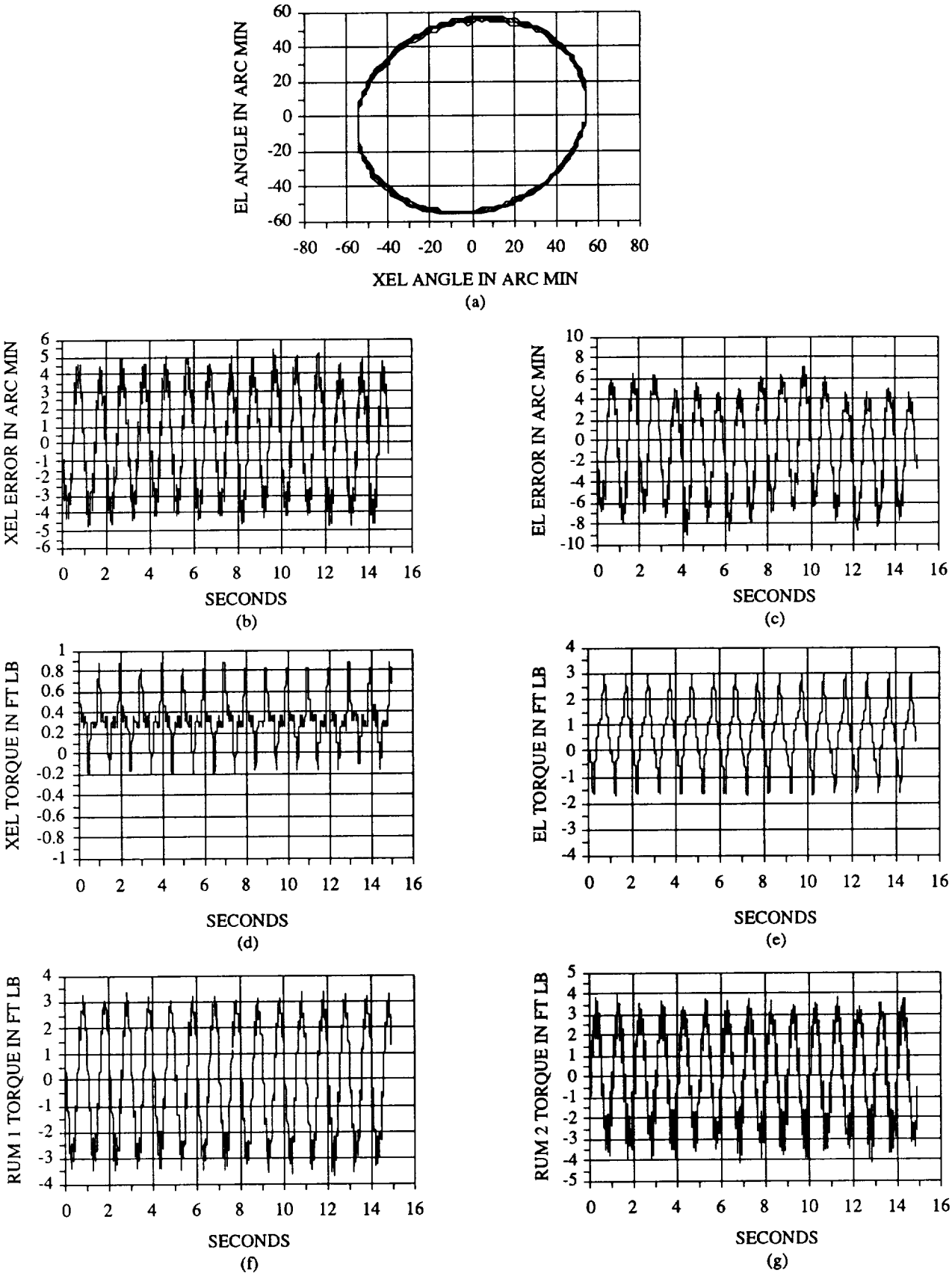

Figure 14. RUM experiment test results for circular scanning with RUM's and gimbal servos at 0° elevation angle.

Table 2. Summary of results from RUM experiment for circular scanning.

EL ANGLE, IN DEG	CMD/ACTUAL SCAN RADIUS, IN ARC-MIN	XEL/EL SCAN ERRORS, IN ARC-MIN RMS[2]	TOTAL POWER FOR TRQ MOTORS USED, IN WATTS RMS[3]
HEADINGS FOR COLUMNS:			
RESULTS USING RUM's AND GIMBAL SERVOS:			
0	51/55[1] (51/51)	3/4 (2/2)	32 (21)
-90	51/55 (51/51)	4/4 (2/2)	4 (<1)
RESULTS USING GIMBAL SERVOS ONLY:			
0	51/18 (51/22)	42/48 (42/42)	147 (99)
0	128/51[4] (128/51)	105/120[4] (105/105)	919[4] (666)
-90	51/20 (51/22)	42/44 (42/42)	144 (99)
-90	128/51[4] (128/51)	105/110[4] (105/105)	900[4] (666)

NOTES:
(1) Top numbers without parentheses are actual hardware results; lower numbers in parentheses are computer simulation results.
(2) Scan errors are error signals in gimbal servos.
(3) Assumes that bias torques of gimbal torque motors can be canceled by better mass balancing.
(4) Extrapolated from result above, based on simulation findings. This is necessary because scan cannot be generated with 11 ft-lb gimbal torque motors that are in RUM experiment.

generate the circular scan at 0° elevation angle reduces the RMS scan error in each axis by a factor of 26 or more and reduces the total torque motor power by a factor of 29. The required peak gimbal torque is reduced from around 22 ft-lb to approximately 4 ft-lb; thus, the size of the gimbal torque motors can be reduced by a factor of 5 or more. The benefits of smaller gimbal motors were stated in section V.

This same methodology was repeated at an elevation angle of –90°. At this orientation, the results for scanning with RUM's are shown in figures 17 and summarized in table 2. The results show that a 55 arc-min radius circular scan is generated. The scan errors are 4 arc-min RMS in each axis and the total motor power is 4 watts RMS. The simulation results for this same case are shown in figure 18 and summarized in table 2. It is important to notice that the simulation results compare well with the actual test results.

Attempting the same scan with the gimbal servos only, as shown in figure 19, generates a 20 arc-min radius circular scan, which does not wander in this case. The scan errors are 42 arc-min RMS or more in each axis and the total motor power is 144 watts RMS. Extrapolating these results, like before, gives a 51 arc-min radius circular scan that has a scan error of 105 arc-min RMS or more in each axis and a total motor power of 900 watts RMS. Again these results are obtained when the gimbal servo commands are increased by a factor of 2.5 and the gimbal torque motors are doubled in size.

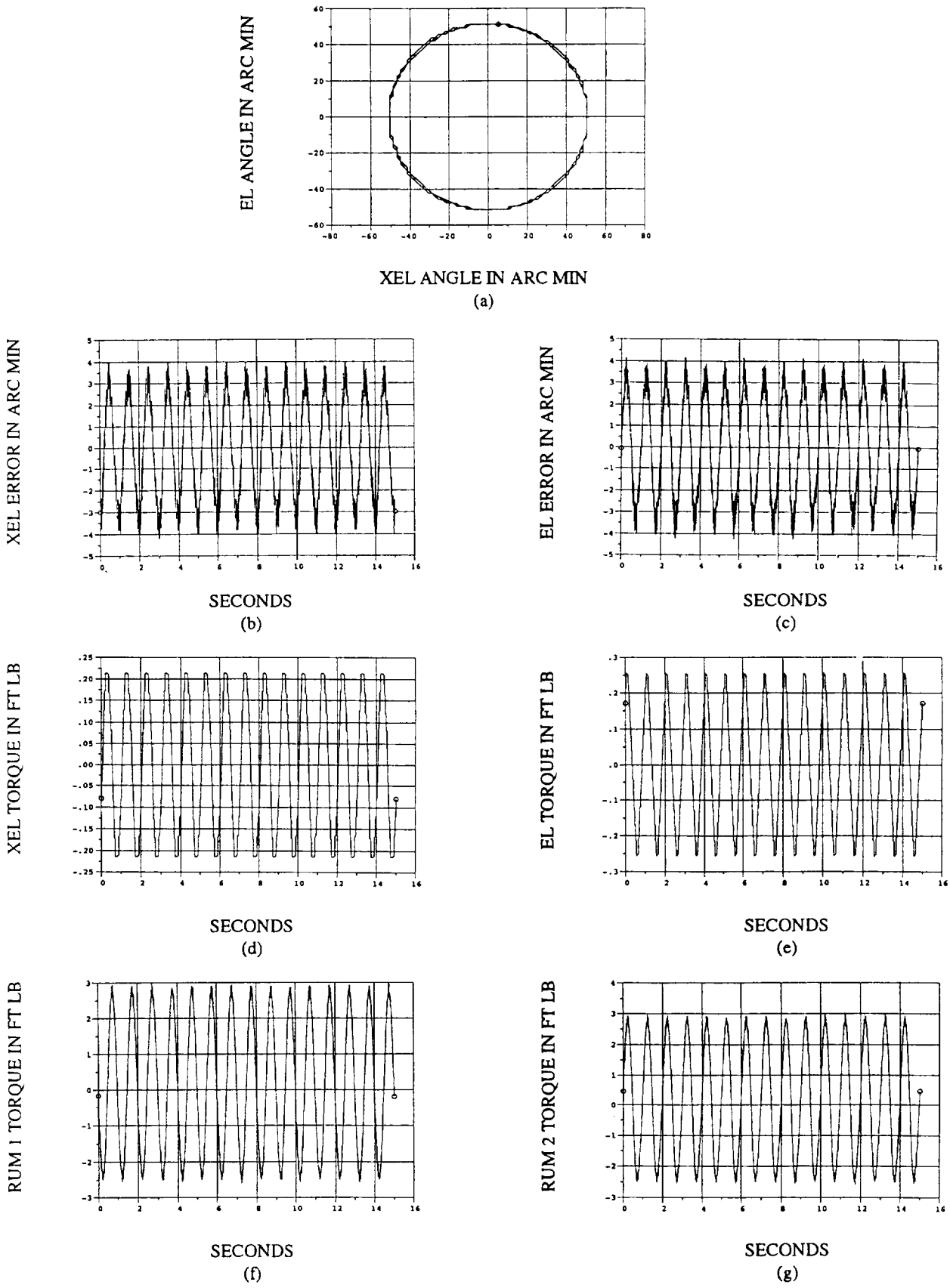

Figure 15. Computer simulation results for circular scanning with RUM's and gimbal servos at 0° elevation angle.

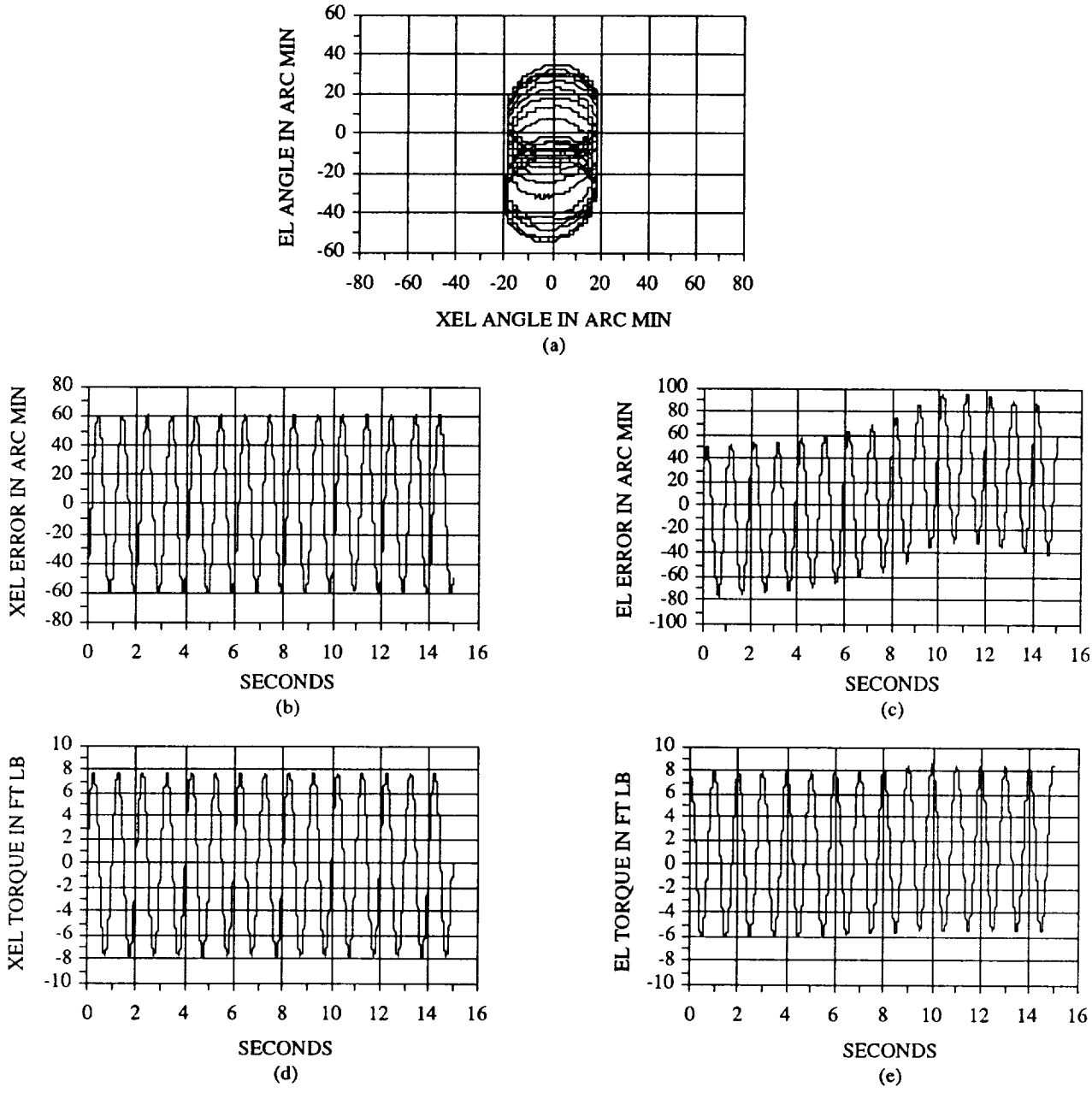

Figure 16. RUM experiment test results for circular scanning with gimbal servos only at 0° elevation angle.

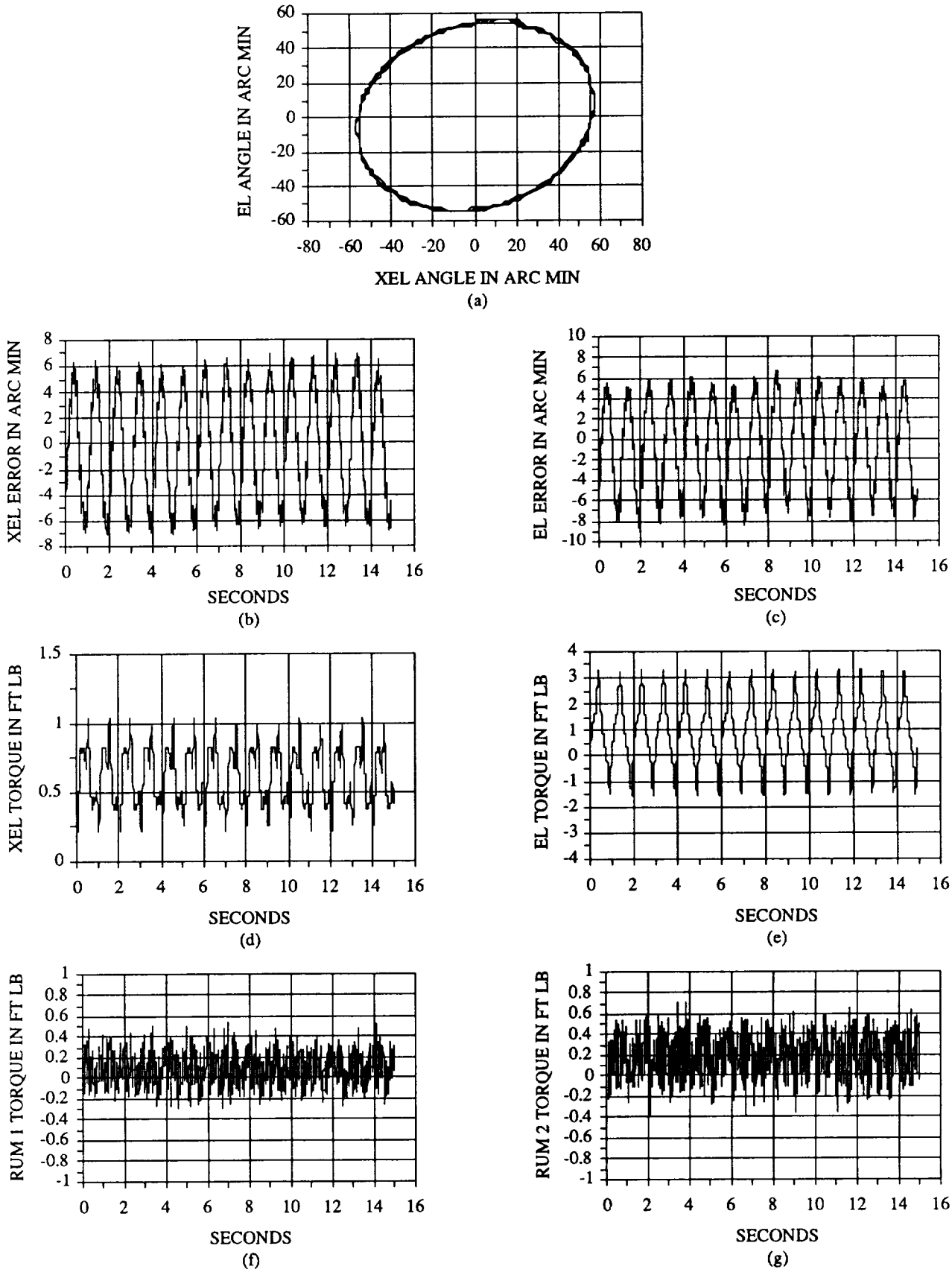

Figure 17. RUM experiment test results for circular scanning with RUM's and gimbal servos at –90° elevation angle.

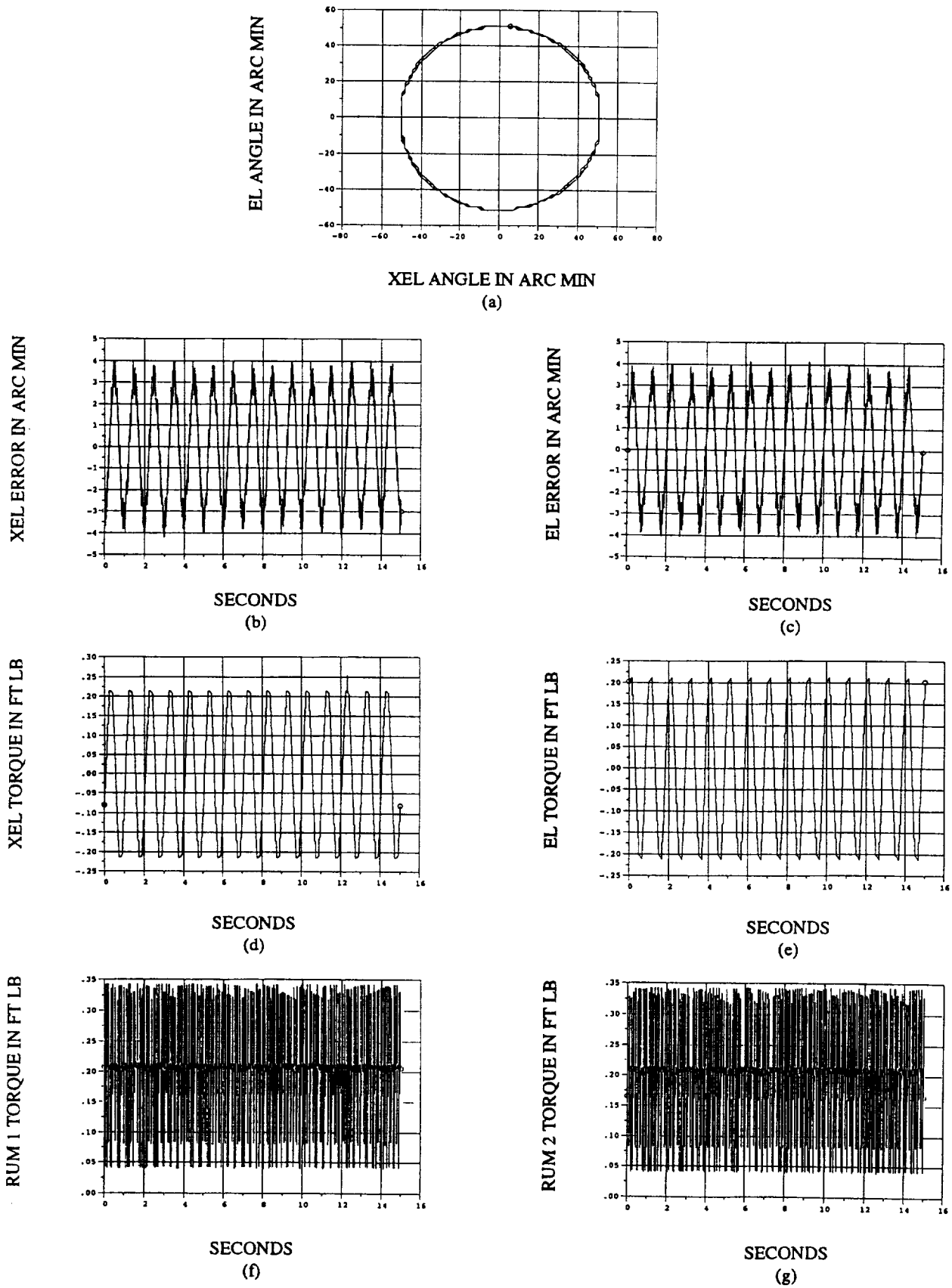

Figure 18. Computer simulation results for circular scanning with RUM's and gimbal servos at –90° elevation angle.

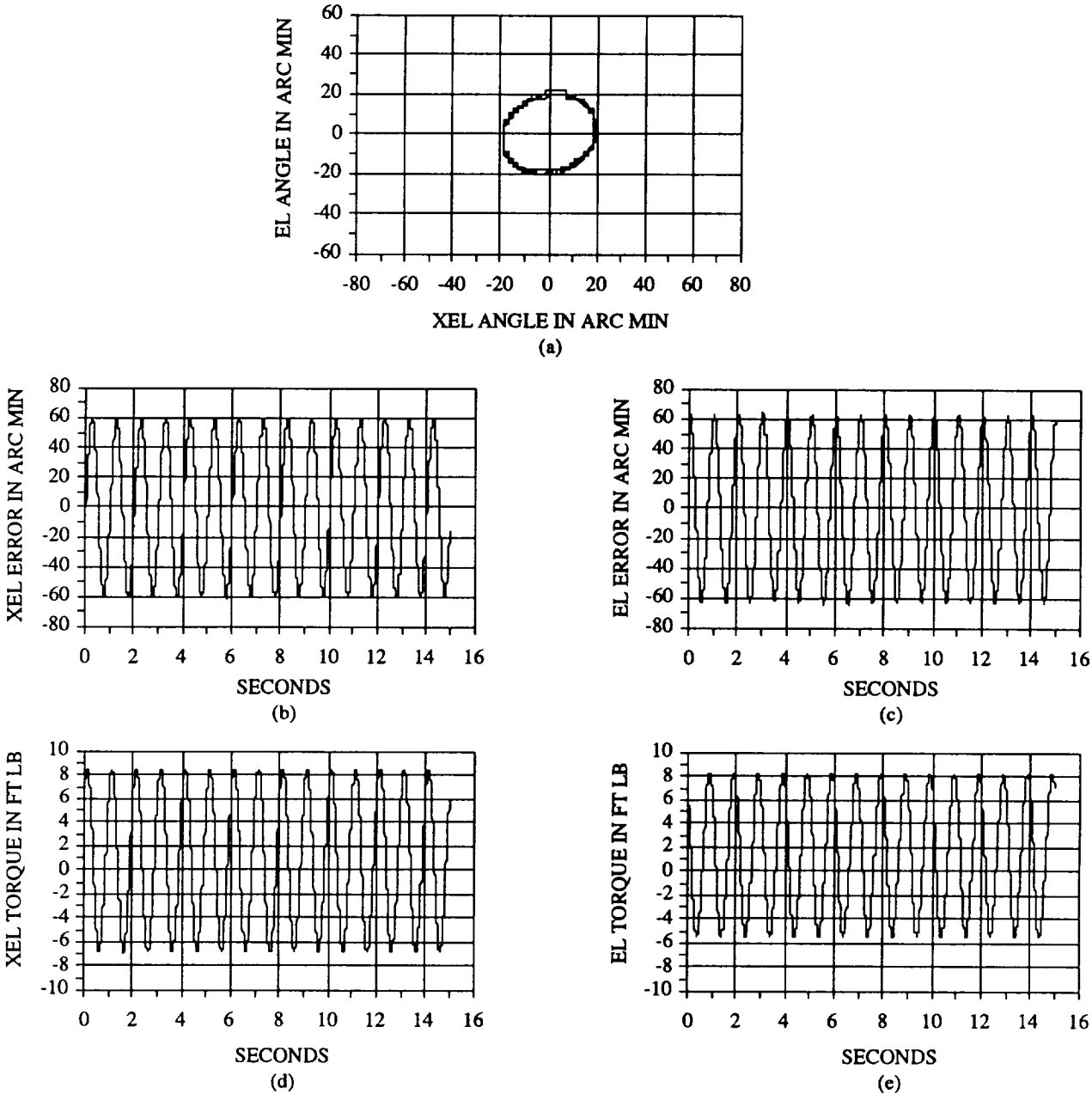

Figure 19. RUM experiment test results for circular scanning with gimbal servos only at –90° elevation angle.

Therefore, using the RUM's to help generate the same approximate scan at a -90° elevation angle reduces the RMS scan error in each axis by a factor of 26 or more and reduces the total motor power by a factor of 225. The peak torque required of the gimbal motors can be reduced from about 22 ft-lb to about 4 ft-lb. Thus, the size of the gimbal motors can be reduced by a factor of 5 or more, which offers the same benefits previously enumerated. Again, it is emphasized that these are the improvements at a 1 sec scan period.

At smaller scan periods, the improvements are even greater when the RUM's are used for circular scanning. Without the RUM's, each time the scan period is divided by 2, both the cross-elevation and the elevation motors need to generate 4 times more torque and dissipate 16 times more power to produce the same sized circular scan. These changes can be proven by the same argument used for linear scanning. Only now, the argument applies to both the cross-elevation and the elevation axes. Thus, each time the scan period is decreased by a factor of 2, the power dissipated in the gimbal motors increases by a factor of 16, when only the gimbal servos are used for circular scanning. Using the same argument as before, the power required to circular scan with RUM's is virtually independent of the scan period.

Again, it is apparent that scanning large payloads at high frequencies without RUM's can require huge gimbal motors that consume too much power to be practical. For example, using gimbal servos only to generate a 51 arc-min radius circular scan with a 0.25 sec period requires gimbal motors with about 350 ft-lb of peak torque. These motors would have to dissipate a total power that exceeds 230 kW of RMS power when scanning in either one-g or zero-g. When RUM's are used to generate the same circular scan, gimbal motors with 4 ft-lb peak torque can be used and the total motor power would be around 32 watts RMS or less in one-g and 1 watt RMS in zero-g.

VII. CONCLUSIONS AND COMMENTS

This experiment has proven a new technology for scanning space-based, balloon-borne, and ground-based gimbaled payloads, as well as free-flying spacecraft. The test results prove that RUM devices can be used to generate accurate linear and circular scans for gimbaled payloads in zero-g and one-g, with very little power. An auxiliary control system is needed to center the scan, and produce some complementary motion when raster scanning. Also, extending the results presented here to free-flying spacecraft is straightforward.

Since the results from the simplified computer simulation model of the RUM experiment agreed fairly well with the results from the actual RUM experiment, the basic theory of scanning with RUM devices is verified. This allows the results presented here to be scaled for larger and smaller payloads scanning at higher and lower frequencies.

Basically, the RUM experiment showed that a pair of RUM's with 5 lb masses on 6 inch lever arms can generate a ±51 arc-min linear scan with a 5 ft long, 250 lb gimbaled payload. Generating this scan without RUM's increases the required motor power by a factor of 17 to 494 in one-g and a factor of 494 in zero-g, at a 1 sec scan period. Furthermore, the size of the gimbal motor in the scan axis increases by a factor of 5.

When the RUM's are used and the scan period is changed, the total motor power and the size of the gimbal motors are unaffected. However, without the RUM's, each time the scan period is reduced by a factor of 2, the motor power increases by an additional factor of 16 and the gimbal motor in the scan axis increases by an additional factor of 4. The increased motor power adversely affects the mass of the electrical power system and a larger gimbal motor requires a stiffer and more massive base structure to react against.

Also, the RUM experiment showed that the same identical RUM devices, mounted for circular scanning, can generate a 55 arc-min radius circular scan with the same gimbaled payload. Generating this scan without the RUM's increases the required motor power by a factor of 29 to 225 in one-g and a

factor of 225 in zero-g, at a 1 sec scan period. In this case, both gimbal motors have to be about five times larger.

When the RUM's are used and the scan period is changed, the total motor power and the size of the gimbal motors are unaffected. However, without the RUM's, each time the scan period is reduced by a factor of 2, the motor power increases by an additional factor of 16 and the size of both gimbal motors increases by a factor of 4.

Furthermore, the gimbal motors are more likely to wear out sooner when they must continuously accelerate and decelerate the payload. The increased power dissipation also generates more internal heat, which affects performance and shortens life expectancy. When the RUM's are used, the gimbal motors work very little and the RUM's rotate at a constant velocity, so all of the motors should have a long life-time.

This experiment proves that it is now feasible to accurately and reliably scan large payloads at high frequencies with significantly less power and significantly less mass, when RUM's generate the basic scan motion. Furthermore, since scanning with RUM's is not founded on torquing against a base structure, it also means that large payloads can scan at high frequencies in places where this was once impossible. For example, consider balloon-borne payloads or free-flying spacecraft.

As a result of this experiment, RUM's are now a proven technology that have known applications in space and have potential applications in defense, industry, and medicine. For example, RUM's may have potential application in military fire control systems for scanning guns. In industry, they have potential applications in spraying water for fighting forest fires or spraying liquid fertilizers and pesticides in open fields. RUM's require so little power that batteries or solar cells could be used as an energy source in remote locations. Also, RUM's could be used in spray painting with a fragile robot arm, because they generate virtually no reaction torques on the arm. In medicine, they may be used for precisely scanning medical devices with considerably less power.

REFERENCES

1. Nein, M.E., and Nicaise, P.D.: "Experiment Pointing Subsystems (EPS) Requirements for the Spacelab Missions." NASA TM X-64978, NASA Marshall Space Flight Center, AL, December 1975.

2. "The GRID on a Balloon Definition Study Report." NASA Goddard Space Flight Center, Greenbelt, MD, June 14, 1989.

3. "Space Telescope Moving Target and Scan Pointing Capability Error Budget, ST/SE-24, Section H, Part 4." LMSC/FO61415, Lockheed Missiles and Space Company, Sunnyvale, CA, October 21, 1985.

4. Polites, M.E.: "Rotating-Unbalanced-Mass Devices for Scanning Balloon-Borne Experiments, Free-Flying Spacecraft, and Space Shuttle/Space Station Experiments." NASA TP-3030, NASA Marshall Space Flight Center, AL, June 1990.

5. Polites, M.E.: "New Method for Scanning Spacecraft and Balloon-Borne/Space-Based Experiments." *Journal of Guidance, Control and Dynamics*, vol. 14, No. 3, May–June 1991, pp. 548–553.

6. Polites, M.E.: "Rotating-Unbalanced-Mass Devices and Methods for Scanning Balloon-Borne-Experiments, Free-Flying Spacecraft, and Space Shuttle/Space Station Attached Experiments," U.S. Patent No. 5,129,600, National Aeronautics and Space Administration, Washington, DC, July 14, 1992.

7. Polites, M.E. and Alhorn D.C.: "Suspension System for Gimbal Supported Scanning Payloads," U.S. Patent Application No. 08/123629, National Aeronautics and Space Administration, Washington, DC, September 15, 1993.

8. Lightsey, W.D., Alhorn, D.C., and Polites, M.E.: "Definition and Design of an Experiment to Test Raster Scanning With Rotating Unbalanced-Mass Devices on Gimballed Payloads." NASA TP-3249, NASA Marshall Space Flight Center, AL, June 1992.

9. Polites, M.E. and Alhorn, D.C.: "Reconfiguring the RUM Experiment to Test Circular Scanning With Rotating Unbalanced-Mass Devices on Gimballed Payloads." NASA-TP-3282, NASA Marshall Space Flight Center, AL, September 1992.

10. "SIRTF at Higher Altitudes," internal document prepared by the Program Development Directorate, NASA Marshall Space Flight Center, AL, December 1987.

☆ U.S. GOVERNMENT PRINTING OFFICE 1994–533-108/00016

REPORT DOCUMENTATION PAGE

Form Approved
OMB No. 0704-0188

1. AGENCY USE ONLY (Leave blank)	2. REPORT DATE	3. REPORT TYPE AND DATES COVERED
	January 1994	Technical Paper

4. TITLE AND SUBTITLE
Results of a Laboratory Experiment That Tests Rotating Unbalanced-Mass Devices for Scanning Gimbaled Payloads and Free-Flying Spacecraft (CDDF Final Report No. 92-02)

5. FUNDING NUMBERS

6. AUTHOR(S)
D.C. Alhorn and M.E. Polites

7. PERFORMING ORGANIZATION NAME(S) AND ADDRESS(ES)
George C. Marshall Space Flight Center
Marshall Space Flight Center, Alabama 35812

8. PERFORMING ORGANIZATION REPORT NUMBER
M-741

9. SPONSORING/MONITORING AGENCY NAME(S) AND ADDRESS(ES)
National Aeronautics and Space Administration
Washington, DC 20546

10. SPONSORING/MONITORING AGENCY REPORT NUMBER
NASA TP-3458

11. SUPPLEMENTARY NOTES
Prepared by Astrionics Laboratory and the Structures and Dynamics Laboratory, Science and Engineering Directorate

12a. DISTRIBUTION/AVAILABILITY STATEMENT
Unclassified—Unlimited
Subject Category: 31

12b. DISTRIBUTION CODE

13. ABSTRACT *(Maximum 200 words)*

Rotating unbalanced-mass (RUM) devices are a new way to scan space-based, balloon-borne, and ground-based gimbaled payloads, like x-ray and gamma-ray telescopes. They can also be used to scan free-flying spacecraft. Circular scans, linear scans, and raster scans can be generated. A pair of RUM devices generates the basic scan motion and an auxiliary control system using torque motors, control moment gyros, or reaction wheels keeps the scan centered on the target and produces some complementary motion for raster scanning. Previous analyses and simulation results show that this approach offers significant power savings compared to scanning only with the auxiliary control system, especially with large payloads and high scan frequencies. However, these claims have never been proven until now. This paper describes a laboratory experiment which tests the concept of scanning a gimbaled payload with RUM devices. A description of the experiment is given and test results that prove the concept are presented. The test results are compared with those from a computer simulation model of the experiment and the differences are discussed.

14. SUBJECT TERMS	15. NUMBER OF PAGES
circular scanning, free-flying spacecraft, gimbaled payloads, laboratory experiment, linear scanning, raster scanning, rotating unbalanced-mass devices, RUM devices	35
	16. PRICE CODE: A03

17. SECURITY CLASSIFICATION OF REPORT	18. SECURITY CLASSIFICATION OF THIS PAGE	19. SECURITY CLASSIFICATION OF ABSTRACT	20. LIMITATION OF ABSTRACT
Unclassified	Unclassified	Unclassified	Unlimited